Accepted by IEEE PES General Meeting 2024

Physics-Data-Driven Power Flow Linearization Considering Topological Remedial Actions

Aline Scherrer*†, Georgia Pierrou*, Mengshuo Jia*, Marc Hohmann†, Gabriela Hug*
*Power Systems Laboratory, ETH Zurich, Zurich, Switzerland
†Swissgrid AG, Aarau, Switzerland
{aline.scherrer, marc.hohmann}@swissgrid.ch, {gpierrou, menjia, ghug}@ethz.ch

***Abstract*—This paper proposes a novel physics-data-driven method for the linearization of AC power flow equations in the context of topological remedial actions. As opposed to physics-based works, the proposed method does not require the re-establishment of the linear model to follow the system changes induced by remedial actions, such as line switching and phase shifting angle variations. By ingeniously leveraging physics-driven aspects, such as hierarchical topology clustering, as well as data-driven regression, the proposed approach can establish a linear mapping between power flows and remedial actions and estimate the new operating point in the event of a remedial action with high accuracy and computational efficiency. Numerical results on a real-world European power network demonstrate the effectiveness of the proposed physics-data-driven linear power flow method in a practical setting. Particularly, the proposed method outperforms purely physics-driven and data-driven methods when a topological remedial action occurs.**

***Index Terms*—power flow, phase shifting transformer, remedial action, topology clustering**

I. Introduction

Modern power grids are characterized by increasing complexity as a result of major transformations, including the rising decentralization through renewable energy supply and the internationalization of the power market [1]. To enhance grid reliability in light of unpredictable fluctuations of renewable generation, the deployment of necessary remedial actions as real-time preventive measures has significantly increased [2]. In particular, remedial actions, such as topological switching or control of the Phase Shifting Transformer (PST) angle have been widely adopted in practice due to their cost-effectiveness, inducing real-time changes in branch impedances and the overall topology of the targeted network [3].

Remedial actions have a substantial effect on the analysis and operation of power grids, including the linearization of the power flow. Yet, they are determined by operators based on experience and their impact is rarely considered in Linearized Power Flow (LPF) models [4]. In particular, linearization techniques that are physics-driven lack the ability to account for frequent topological changes introduced by remedial actions in an efficient manner. Such formulation would require a re-establishment of the linear model to follow the system changes induced by remedial actions, creating a considerable computational burden [5]. Although data-driven LPF models that reduce the dependency on the network model have been proposed [6], [7], remedial actions are not considered.

Limited work has been done to effectively integrate remedial actions in LPF models. In [8], a decoupled LPF model that integrates the PST influence in the admittance matrix and branch flows is proposed. A linear representation of preventive and corrective actions, including PST control and switching, in an Optimal Power Flow (OPF) is presented in [9]. However, a computationally efficient and practically feasible LPF method that can accurately map topological changes and PST angle variations as controllable variables to power flow states in the context of remedial actions is still missing.

In this paper, an *online hybrid physics- and data-driven*, i.e., physics-data-driven LPF model is proposed. Aiming to integrate the real-time influence of remedial actions in the LPF formulation, the proposed approach leverages the physics-based model along with data-driven estimation to achieve satisfactory computational efficiency and accuracy in the context of LPF under remedial actions. The novelty and the main contributions of the work are given as follows:

- To seamlessly take remedial actions into account and eliminate the need for re-establishing the linear model, the proposed approach integrates topology switching and PST angles as controllable variables of the LPF model. To the best of our knowledge, this is the first time that parameters related to common remedial schemes are directly treated as controllable variables in LPF studies.
- A data-driven regression analysis is proposed to find a linear mapping between remedial actions and power flow states and efficiently estimate new operating points under altered topologies induced by remedial actions.
- A physics-driven hierarchical topology clustering technique is included in the data-driven scheme to enable network partitioning and reduce computational time.
- A comprehensive numerical study on a real-world European power network consisting of more than 10,000 buses demonstrates the practical feasibility and computational efficiency of the proposed method.

The remainder of the paper is organized as follows: Section II provides the physics-driven formulation under topological remedial actions. In Section III, the proposed physics-data-driven LPF algorithm considering topological remedial actions is discussed. In Section IV, the proposed method is validated in a case study. Section V summarizes the conclusions and

This work was supported by the Swiss National Science Foundation under CRSK-2_221126/1 (Corresponding author: Mengshuo Jia).

gives perspectives for future work.

II. Physics-driven Model Under Remedial Actions

This section reviews the impact of remedial actions from a physics-driven perspective. An extended version of the power flow model that integrates topological remedial actions, including the use of PSTs, is described in detail.

A. Integration of Remedial Actions

The well-known power flow equations describing the active and reactive power injections at bus $i, i = 1, ..., n$ are:

$$P_i = V_i \sum_{j=1}^{n} V_j (G_{ij} \cos\theta_{ij} + B_{ij} \sin\theta_{ij}) \quad \forall i \tag{1}$$

$$Q_i = V_i \sum_{j=1}^{n} V_j (G_{ij} \sin\theta_{ij} - B_{ij} \cos\theta_{ij}) \quad \forall i \tag{2}$$

where P_i and Q_i are the net active and reactive power injections at bus i, respectively, G_{ij} and B_{ij} are elements of the real and imaginary part of the nodal admittance matrix Y, respectively, V_i is the voltage magnitude of bus i, θ_i is the voltage angle of bus i, θ_{ij} is the voltage angle difference between buses i and j, and n is the number of buses.

To consider the impact of remedial actions in the power flow formulation, the nodal admittance matrix elements that include a model of the PST are given by:

$$Y_{ii} = \sum_{j=1}^{n} (t_{ij}^2 y_{ij} + y_{ij}^{sh}) + y_i^{fxsh} \tag{3}$$

$$\begin{aligned} Y_{ij} = -t_{ij} t_{ji} [&(g_{ij} \cos\delta_{ij} + b_{ij} \sin\delta_{ij}) \\ &+ j(b_{ij} \cos\delta_{ij} - g_{ij} \sin\delta_{ij})] \end{aligned} \tag{4}$$

where $t_{ij}\angle\phi_{ij}, t_{ji}\angle\phi_{ji}$ are the complex tap ratios of the windings connected to buses i, j, respectively, δ_{ij} is defined as the angle difference $\delta_{ij} = -\phi_{ij} + \phi_{ji}$, y_i^{fxsh} is the fixed shunt admittance of bus i, $y_{ij} = g_{ij} + jb_{ij}$ is the branch admittance of the line connecting buses i, j, and y_{ij}^{sh} is the shunt admittance of the line connecting buses i, j. Note that for branches without any transformer, $t_{ij} = 1$ and $\phi_{ij} = 0$.

By substituting the nodal admittance matrix elements (3)-(4) in the power injections (1)-(2), the power flow equations integrating the influence of the PSTs are obtained.

B. Impact of Remedial Actions

Following the integration of the PST impact on the power flows, the nodal power balance mismatches at each bus i can be expressed as a function of voltage magnitudes, voltage angles, and PST angles as:

$$f_i(\boldsymbol{x}, \boldsymbol{\phi}) = S_i^s - S_i(\boldsymbol{x}, \boldsymbol{\phi}) \quad \forall i \tag{5}$$

where $\boldsymbol{x} = [\boldsymbol{V}^T, \boldsymbol{\theta}^T]^T$ is the state vector including the voltage magnitudes $\boldsymbol{V}$ and voltage angles $\boldsymbol{\theta}$, $\boldsymbol{\phi}$ is a vector including the PST angles, S_i is the calculated apparent power injection, S_i^s is the specified apparent power injection at bus i.

Next, by applying the first-order Taylor approximation to the nodal power mismatch equations around the operating point $\boldsymbol{x}_0 = [\boldsymbol{V}_0^T, \boldsymbol{\theta}_0^T]^T$ and PST angles $\boldsymbol{\phi}_0^T$, we have:

$$\begin{aligned} f_i^P(\boldsymbol{x}, \boldsymbol{\phi}) \;=\; & P_i^s - P_i(\boldsymbol{x}_0, \boldsymbol{\phi}_0) - \nabla_{\boldsymbol{x}}^T P_i(\boldsymbol{x}_0, \boldsymbol{\phi}_0)(\boldsymbol{x} - \boldsymbol{x}_0) \\ & - \nabla_{\boldsymbol{\phi}}^T P_i(\boldsymbol{x}_0, \boldsymbol{\phi}_0)(\boldsymbol{\phi} - \boldsymbol{\phi}_0) \quad \forall i \end{aligned} \tag{6}$$

$$\begin{aligned} f_i^Q(\boldsymbol{x}, \boldsymbol{\phi}) \;=\; & Q_i^s - Q_i(\boldsymbol{x}_0, \boldsymbol{\phi}_0) - \nabla_{\boldsymbol{x}}^T Q_i(\boldsymbol{x}_0, \boldsymbol{\phi}_0)(\boldsymbol{x} - \boldsymbol{x}_0) \\ & - \nabla_{\boldsymbol{\phi}}^T Q_i(\boldsymbol{x}_0, \boldsymbol{\phi}_0)(\boldsymbol{\phi} - \boldsymbol{\phi}_0) \quad \forall i \end{aligned} \tag{7}$$

It is worth noting that by solving (6)-(7) $\boldsymbol{\phi}$ is obtained and considered in the same way as $\boldsymbol{x}$, i.e., as an output vector rather than as an input vector that includes controllable variables. Instead, a relationship to derive $\boldsymbol{x}$ based on the power injections and $\boldsymbol{\phi}$ as inputs is desirable. This fact indicates the complexity of deriving an explicit linearized model from the AC model (i.e., the physics-driven linearization) that can accurately map PST angle variations or other topological changes to the power flow solution $\boldsymbol{x}$, as in the case of power injections. As will be shown in the next sections, this paper overcomes this issue using a hybrid physics-data-driven approach.

III. Proposed Accelerated Physics-Data-Driven LPF Under Remedial Actions

Section II has shown the complexity caused by the integration of remedial actions from a physics-driven perspective. In this section, the proposed accelerated physics-data-driven LPF method to conduct the linear mapping of topological remedial actions to the corresponding operating point is presented. By ingeniously leveraging physics-driven hierarchical topology clustering along with data-driven regression, the proposed hybrid physics-data-driven LPF model can provide an accurate and computationally efficient estimation of the operating point under remedial actions.

A. LPF Mapping Under Remedial Actions

To overcome the complexity brought by the consideration of remedial actions in the AC model, a power flow model is formulated to provide the mapping between power injections, remedial actions and the operating point, i.e.,

$$\boldsymbol{x} = \boldsymbol{h}(\boldsymbol{P}^s,\ \boldsymbol{Q}^s,\ \boldsymbol{L},\ \boldsymbol{\phi}) \tag{8}$$

where $\boldsymbol{L}$ represents line status (a.k.a., the flatten incidence matrix), $\boldsymbol{P}^s$ and $\boldsymbol{Q}^s$ are injection set-points, $\boldsymbol{\phi}$ refers to the PST angles, and $\boldsymbol{x}$ (including $\boldsymbol{\theta}$, and $\boldsymbol{V}$) denotes the power flow state. The mapping direction considered is in accordance with the procedure of the deployment of remedial actions, where the PST angles $\boldsymbol{\phi}$ or the lines to be switched are known and $\boldsymbol{\theta}, \boldsymbol{V}$ are to be calculated. Thus, (8) ingeniously takes power injections and remedial actions, such as line switching and PST angle variations, as controllable variables. In the next step, we linearize (8).

B. PLS Regression

To extract the LPF model from (8), the generalized regression equation is formulated using the datasets of $\boldsymbol{x}$ and $\boldsymbol{P}^s, \boldsymbol{Q}^s, \boldsymbol{L}, \boldsymbol{\phi}$. Assuming $Z \in \mathbb{R}^{N_Z \times N_s}$ includes N_s samples of the independent variables, i.e., $\boldsymbol{P}^s, \boldsymbol{Q}^s, \boldsymbol{L}, \boldsymbol{\phi}$, $X \in \mathbb{R}^{N_X \times N_s}$

includes N_s samples of dependent variables, i.e., $\boldsymbol{x}$, and β is the regression parameter matrix, we have:

$$X = \beta Z \tag{9}$$

Once the sufficient and representative window of samples is included in Z, X, Partial Least Squares (PLS) regression is applied to find β [10], [11]. Beyond traditional Least Squares regression which falls short in addressing practical complexities, PLS regression has demonstrated effectiveness in managing collinearity of data and overfitting [10], [11]. Specifically, PLS decomposes Z, X into N_p components by

$$Z = CT^T + E \tag{10}$$

$$X = RU^T + F \tag{11}$$

where $T \in \mathbb{R}^{N_s \times N_p}$ and $U \in \mathbb{R}^{N_s \times N_p}$ consist of N_p components extracted from Z and X, called score components; $C \in \mathbb{R}^{N_Z \times N_p}$ and $R \in \mathbb{R}^{N_X \times N_p}$ denote the so-called loading matrices of Z and X so that the scores form an orthogonal basis; $E \in \mathbb{R}^{N_Z \times N_s}$ and $F \in \mathbb{R}^{N_X \times N_s}$ represent the matrices of residuals for Z and X. Finally, the solution to (9) is:

$$\hat{\beta} = Z^T U \left(T^T Z Z^T U\right)^{-1} T^T X \tag{12}$$

C. Accelerated PLS Regression with Topology Clustering

Sections III-A, III-B have shown that PLS regression can establish a linear data-driven mapping of topological remedial actions to the corresponding operating point and power flows. However, directly using the PLS regression on a complete network model is computationally challenging due to the scale of the system, especially for large systems. To overcome the computational complexity, an accelerated PLS regression on the basis of hierarchical topology clustering is proposed.

In fact, assuming that a remedial scheme, e.g., topology variation, occurs, it is expected that only specific groups of buses of a large network will be affected non-negligibly. Thus, applying a clustering algorithm to a power system network can enhance the regression analysis in the context of remedial actions, as it reduces network complexity and facilitates the selection of appropriate or crucial actions.

In this work, hierarchical clustering is embedded in the PLS regression. Briefly speaking, the concept of electrical distances is applied to identify bus coupling and divide a power system network into clusters [12]. It is worth noting that the network partitioning procedure is done offline and it is flexible, as no a priori specification of the number of clusters is needed.

1) Electrical Distance: The calculation of the electrical distance is based on the matrix $\frac{\partial \boldsymbol{Q}}{\partial \boldsymbol{V}}$ which is a part of the power flow Jacobian [12]. By taking its inverse $\frac{\partial \boldsymbol{V}}{\partial \boldsymbol{Q}}$, the attenuation a_{ij} reflecting the voltage coupling between buses i and j can be computed as follows:

$$a_{ij} = \frac{\partial V_i}{\partial Q_j} / \frac{\partial V_j}{\partial Q_j} \quad \forall i, j \tag{13}$$

and

$$\Delta V_i = a_{ij} \Delta V_j \quad \forall i, j \tag{14}$$

To ensure matrix symmetry, the electrical distance d_{ij} between buses i and j is defined and normalized to obtain values in the range between 0 and 1 as:

$$d_{ij} = d_{ji} = -\log(a_{ij} \cdot a_{ji}) \tag{15}$$

$$d_{ij} = \frac{d_{ij}}{\max(d_{i1}, ..., d_{in})} \tag{16}$$

It should be highlighted that a small value of the electrical distance signifies a strong coupling between buses i, j, i.e., buses i, j should be grouped within the same cluster.

2) Agglomerative Hierarchical Clustering: Once the electrical distances between all pairs of buses i, j are calculated, the Agglomerative Hierarchical Clustering (AHC) algorithm is applied [13]. Initially, each bus forms an independent cluster. Subsequently, an iterative merging process of similar clusters is deployed until one cluster or m desired clusters are formed. The maximum electrical distances between buses in the different clusters are utilized as the merging criteria at each iteration, i.e., the two clusters where the minimum among the maximum electrical distances is observed are merged into a new cluster. The resulting dendrogram visually portrays the cluster hierarchy and can be used to determine the number of considered clusters m. Finally, buses are grouped into specific clusters, denoted as C_l for $l \in \{1, \ ... \ , m\}$.

3) Accelerated PLS Sample Generation: In this work, samples are generated offline by modifying power injections and topology through line switching or PST angle variations and computing and storing the corresponding operating point. To improve efficiency and accelerate PLS regression, samples are partitioned into clusters, i.e., we collect the sample vectors $\hat{\boldsymbol{\zeta}}_{C_l}^{(k)}, k = 1, ..., N_s$ including the topological remedial actions and the sample vectors $\hat{\boldsymbol{x}}_{C_l}^{(k)}$ including the operating points, for each cluster $C_l, l = 1, ..., m$ as follows:

$$\hat{\boldsymbol{\zeta}}_{C_l}^{(k)} = [\hat{\boldsymbol{P}}_{C_l}^{s,(k)^T}, \hat{\boldsymbol{Q}}_{C_l}^{s,(k)^T}, \hat{\boldsymbol{L}}_{C_l}^{(k)^T}, \hat{\boldsymbol{\phi}}_{C_l}^{(k)^T}]^T \quad \forall k, C_l \tag{17}$$

$$\hat{\boldsymbol{x}}_{C_l}^{(k)} = [\hat{\boldsymbol{V}}_{C_l}^{(k)^T}, \hat{\boldsymbol{\theta}}_{C_l}^{(k)^T}]^T \quad \forall k, C_l \tag{18}$$

Hence, by collecting the sample data matrices for each cluster, i.e., $Z_{C_l} = [\hat{\boldsymbol{\zeta}}_{C_l}^{(1)} ... \hat{\boldsymbol{\zeta}}_{C_l}^{(k)} ... \hat{\boldsymbol{\zeta}}_{C_l}^{(N_s)}]$ and $X_{C_l} = [\hat{\boldsymbol{x}}_{C_l}^{(1)} ... \hat{\boldsymbol{x}}_{C_l}^{(k)} ... \hat{\boldsymbol{x}}_{C_l}^{(N_s)}]$, an accelerated PLS regression scheme can be applied and solved for each cluster using (12) as:

$$\hat{\beta}_{C_l} = Z_{C_l}^T U_{C_l} \left(T_{C_l}^T Z_{C_l} Z_{C_l}^T U_{C_l}\right)^{-1} T_{C_l}^T X_{C_l} \quad \forall l \tag{19}$$

D. Proposed Physics-Data-Driven LPF Algorithm

A flowchart of the proposed physics-data-driven LPF model in the context of remedial actions is illustrated in Fig. 1. **Steps 1–6** constitute the offline phase, where the PST integration, topology clustering process and the accelerated PLS regression model training are conducted. **Steps 7–8** correspond to the online phase, where the proposed LPF model computes the estimated operating point in the event of a topological remedial action.

Remarks: In the PLS regression training process, there is a trade-off between creating an indicative dataset with a balanced representation across the clusters while keeping the accuracy and the number of samples in a reasonable range. Although the combination of remedial actions to be reflected in

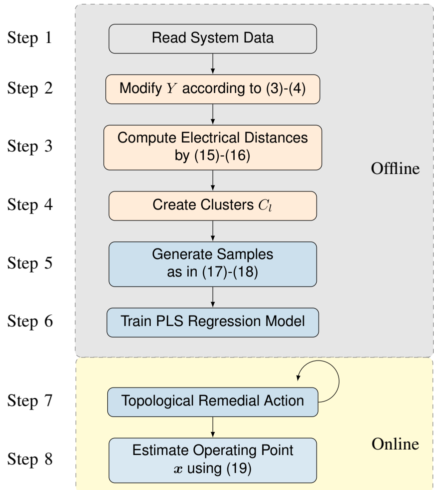

Fig. 1: Flowchart of the proposed physics-data-driven LPF.

the input data can be very high, the issue can be addressed by either collecting as samples available results from simulations or metering devices [14], or by focusing on specific topologies, as typically done in realistic case studies [15].

IV. Numerical Results

In this section, numerical results of the proposed physics-data-driven LPF model under remedial actions are presented. First, the results of the offline phase, including clustering and PLS regression training, are provided. Next, the online phase of the proposed approach is validated and its performance is compared to purely physics-driven or data-driven methods.

A. Network Model

A modified version of the real-world European power network model provided by Swissgrid AG, the Swiss Transmission System Operator, is utilized to demonstrate the performance of the proposed method. The extensive network consists of more than 11,000 busbars connected through over 18,000 branch connections, and over 3,000 transformers. Around 150 of those are modeled as PSTs (**Steps 1-2**). The implementation is carried out in Python in combination with Power System Simulator for Engineering (PSS®E) by Siemens [16].

B. Offline Topological Clustering and PLS Regression Results

To reduce the network complexity under remedial actions and enhance the computational efficiency of the PLS regression training, the hierarchical clustering based on electrical distances is applied (**Steps 3-4**). The resulting dendrogram reflecting the different clusters is shown in Fig. 2. Specifically, four notably large partitions can be observed, with the largest one including 2,498 buses. Note that selecting clusters that include over 6,000 buses may cause memory errors in the PLS regression, which further highlights the importance of applying techniques like topology clustering in real-world LPF models. Based on this result, the number of clusters is set to $m = 30$.

Next, the PLS cluster-based regression training is conducted (**Steps 5-6**). As highlighted in the Remarks of Section III-D, an equal distribution of topological actions, e.g., line switching and PST angle variations, is implemented to ensure representative samples within each cluster. Inspired by one-dimensional Latin hypercube sampling [17], an iterative sampling process is performed to collect the random samples within each cluster. Branch outages and PST angle variations are randomly selected within each cluster, whereas power injection modifications are applied by scaling the power of generators and loads for each sample.

Table I presents a comparison of the proposed regression approach that integrates topology clustering with the complete regression approach over the entire network where no clustering is considered. Based on the coefficient of determination (R-squared) and the Mean Squared Error (MSE), the proposed cluster-based regression can accurately map remedial actions to the operating point. The proposed approach is also computationally efficient compared to the complete regression approach. Indeed, thanks to the proposed cluster-based method, a significant decrease in the training time of the regression model can be achieved ($\sim$30 minutes are required for the clustered-based PLS regression training, whereas $\sim$14 hours are required for the PLS regression training on the complete network). Hence, although the regression on the complete model achieves higher accuracy in estimating voltage angles, the cluster-based method can effectively reduce the problem scale, allowing for the implementation of the PLS algorithm on smaller subgroups of large practical power systems. It is however important to note that the performances of the two algorithms are likely dependent on the specific system. Nevertheless, for the considered test system, it can be concluded that the accuracies are similar with a clear advantage in terms of computational efficiency for the cluster-based method.

C. Online Physics-data-driven LPF Results

Following the offline successful mapping of topological remedial actions to the operating point through the clustered-based PLS regression, the proposed physics-data-driven LPF method is tested online (**Steps 7-8**). Several topological remedial actions are simulated and the estimated operating point is computed. Since the testing cases can vary depending on the possible combinations of remedial actions, we present the results for 30 topological remedial actions of interest that commonly occur in real-world grid operations.

To evaluate the performance of the proposed approach, different methods for the calculation of the operating point are considered. Particularly, the result of the proposed physics-data-driven LPF approach is compared to the results of the

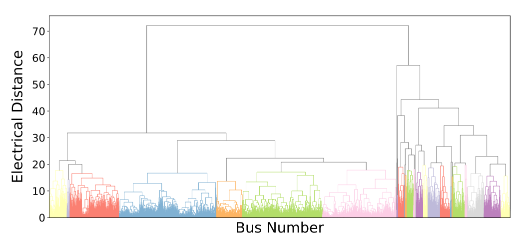

Fig. 2: Topology clustering of the European network.

TABLE I
COMPLETE VS CLUSTER-BASED REGRESSION

Estimation Variables	Complete Regression		Proposed Clustered Regression	
	R-squared	MSE	R-squared	MSE
$\boldsymbol{V}$	0.9998	$2.43 \cdot 10^{-8}$	0.9999	$1.36 \cdot 10^{-8}$
$\boldsymbol{\theta}$	0.9999	$4.61 \cdot 10^{-7}$	0.9998	$3.04 \cdot 10^{-6}$

data-driven complete regression introduced previously as well as to the following physics-driven approaches:

1) Baseline Method: The result of the baseline method is obtained by solving (6), (7), where $\boldsymbol{x_0}$ is the operating point before any remedial action is taken.

2) Average Method: The result of the average method is obtained by solving (6), (7), where $\boldsymbol{x_0}$ is an average of the actual operating points after the topological remedial actions are taken. This method is typically employed in practice to provide a quick estimation of the operating point on the basis of common actions and historical data.

The solver Gurobi [18] is used to compute the result of the Baseline and Average methods. For each method, the computed operating points are compared to the actual ones obtained from the simulation in PSS®E. The results in terms of the estimation error of voltage magnitudes (in %), voltage angles (absolute difference in radians), and current magnitudes $\boldsymbol{I}$ (absolute difference in p.u.), are presented in Table II and Fig 3. The % estimation errors of $\boldsymbol{\theta}, \boldsymbol{I}$ are not defined as many have close to zero values. It can be observed that the proposed approach demonstrates a significantly improved performance in terms of accuracy and outperforms the physics-driven Baseline and Average methods. Moreover, the accuracy of the proposed clustered-based LPF model is similar to the one of the complete data-driven model, yet the performance of the proposed method is superior with respect to computational efficiency. Indeed, as shown in Table III, thanks to the clustering, the proposed approach is four times faster in the online phase. We conclude that the proposed physics-data-driven LPF model can accurately and efficiently predict the new operating points under topological remedial actions and the estimation errors for $\boldsymbol{V}, \boldsymbol{\theta}$ are within expected and acceptable ranges [7].

TABLE II

ESTIMATION ERROR FOR $\boldsymbol{V}, \boldsymbol{\theta}, \boldsymbol{I}$

Estimation Variables	Baseline	Average	Complete	Proposed
$\boldsymbol{V}$	$2.63 \cdot 10^{-1}$	$4.89 \cdot 10^{-2}$	$7.81 \cdot 10^{-4}$	$6.82 \cdot 10^{-4}$
$\boldsymbol{\theta}$	$1.09 \cdot 10^{-3}$	$1.98 \cdot 10^{-4}$	$4.58 \cdot 10^{-4}$	$7.16 \cdot 10^{-4}$
$\boldsymbol{I}$	$1.63 \cdot 10^{-1}$	$7.31 \cdot 10^{-2}$	$6.29 \cdot 10^{-2}$	$6.57 \cdot 10^{-2}$

TABLE III

AVERAGE RUNTIME TO ESTIMATE OPERATING POINTS

Runtime	Baseline	Average	Complete	Proposed
online (s)	2.023	1.930	7.626	1.892

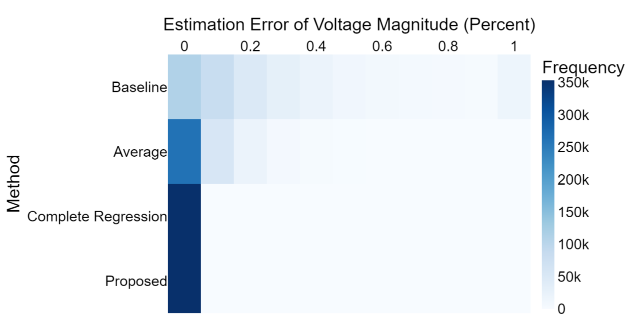

Fig. 3: The % voltage magnitude estimation errors. The proposed hybrid approach outperforms purely physics-driven and data-driven approaches.

V. Conclusion

In this paper, a novel physics-data-driven LPF method considering topological remedial actions is proposed. The proposed approach leverages information embedded in the physics-based model along with data-driven training based on regression to map topological remedial actions and power flow results with high accuracy and computational efficiency. The proposed method represents the first attempt to consider remedial actions, such as line switching and PST angle variation as controllable variables, overcoming the need of re-establishing the linear model under such events. A study on a real-world European grid validates the effectiveness of the proposed method compared to purely physics-driven and data-driven methods when a topological action occurs. Future work may focus on enriching training and testing cases and integrating the proposed approach in remedial action optimization.

References

[1] E. Vrettos, M. Hohmann, M. Zima, “A Vision to enhance Transmission Security: the Case of Switzerland’s Power System,” in *IEEE Power and Energy Magazine*, vol. 19, no. 2, pp. 56-68, 2021.

[2] H. He, E. Du, N. Zhang, C. Kang, X. Wang, “Enhancing the Power Grid Flexibility with Battery Energy Storage Transportation and Transmission Switching,” in *Applied Energy*, vol. 290, pp. 116692, 2021.

[3] E. Little, S. Bortolotti, J. -Y. Bourmaud, E. Karangelos, Y. Perez, “Optimal Transmission Topology for facilitating the Growth of Renewable Power Generation,” in *IEEE PowerTech*, Madrid, Spain, 2021.

[4] M. Hohmann, J. Warrington and J. Lygeros, “Optimal Linearizations of Power Systems With Uncertain Supply and Demand,” in *IEEE Trans. Power Systems*, vol. 34, no. 2, pp. 1504–1512, 2019.

[5] D. A. Contreras, K. Rudion, “Impact of Grid Topology and Tap Position Changes on the Flexibility Provision from Distribution Grids,” in *IEEE PES ISGT Europe*, Bucharest, Romania, 2019.

[6] Z. Shao, Q. Zhai, J. Wu, X. Guan, “Data Based Linear Power Flow Model: Investigation of a Least-Squares based Approximation,” in *IEEE Trans. Power Systems*, vol. 36, no. 5, pp. 4246-4258, 2021.

[7] Y. Liu, Y. Wang, N. Zhang, D. Lu, C. Kang, “A Data-Driven Approach to linearize Power Flow Equations considering Measurement Noise,” in *IEEE Trans. Smart Grid*, vol. 11, no. 3, pp. 2576-2587, 2020.

[8] J. Yang, N. Zhang, C. Kang and Q. Xia, “A State-Independent Linear Power Flow Model with accurate Estimation of Voltage Magnitude,” in *IEEE Trans. Power Systems*, vol. 32, no. 5, pp. 3607-3617, 2017.

[9] T. Van Acker, D. Van Hertem, “Linear Representation of preventive and corrective Actions in OPF Models”, in *Proceedings of the Young Researchers Symposium*, Eindhoven, Netherlands, 2016.

[10] Y. Liu, N. Zhang, Y. Wang, J. Yang, C. Kang, “Data-Driven Power Flow Linearization: A Regression Approach,” in *IEEE Trans. Smart Grid*, vol. 10, no. 3, pp. 2569-2580, 2019.

[11] M. Jia, G. Hug, N. Zhang, Z. Wang, Y. Wang, “Tutorial on data-driven power flow linearization-part i: Challenges and training algorithms,” [Online]. Available: https://www.research-collection.ethz.ch/handle/20.500.11850/606654

[12] J. Zhong, E. Nobile, A. Bose, K. Bhattacharya, “Localized Reactive Power Markets using the concept of Voltage Control Areas,” in *IEEE Trans. Power Systems*, vol. 19, no. 3, pp. 1555-1561, 2004.

[13] V. Alimisis, P. C. Taylor, “Zoning Evaluation for improved Coordinated Automatic Voltage Control,” in *IEEE Trans. Power Systems*, vol. 30, no. 5, pp. 2736–2746, 2015.

[14] J. Chen, W. Wu and L. A. Roald, “Data-Driven Piecewise Linearization for Distribution Three-Phase Stochastic Power Flow,” in *IEEE Trans. Smart Grid*, vol. 13, no. 2, pp. 1035–1048, 2022.

[15] A. Marot, B. Donnot, S. Tazi, P. Panciatici, “Expert System for topological remedial action discovery in smart grids”, in *MedPower*, Dubrovnik, Croatia, 2018.

[16] Siemens Industry, Inc., “Program Operation Manual PSSE 35.1.0,” Schenectady, NY, USA, 2020.

[17] We. Loh, “On Latin Hypercube Sampling,” in *The Annals of Statistics*, vol. 24, pp. 2058-2080, 1996.

[18] Gurobi Optimization, LLC, “Gurobi optimizer reference manual,” 2023. [Online]. Available: https://www.gurobi.com